



NIH PUBLIC ACCESS

Author Manuscript

Inflamm Bowel Dis. Author manuscript; available in PMC 2010 December 1.

Published in final edited form as:

Inflamm Bowel Dis. 2009 December ; 15(12): 1794–1802. doi:10.1002/ibd.21018.

Genetic dissection of granulomatous enterocolitis and arthritis in the intramural peptidoglycan-polysaccharide-treated rat model of IBD

A. Bleich, DVM, PhD¹, S. Hopf, DVM¹, H.J. Hedrich, DVM¹, H.A. van Lith, PhD², F. Li, MD³, R. Balfour Sartor, MD^{3,#}, and M. Mähler, DVM^{1,4,#}

¹Institute for Laboratory Animal Science and Central Animal Facility, Hannover Medical School, Hannover, Germany ²Department of Animals, Science and Society, Division of Laboratory Animal Science, Faculty of Veterinary Medicine, and Rudolf Magnus Institute of Neuroscience, Utrecht University, Utrecht, The Netherlands ³Center for Gastrointestinal Biology and Disease, University of North Carolina, Chapel Hill, USA

Abstract

Background & Aim—Inflammatory arthropathies are common extraintestinal manifestations of inflammatory bowel diseases (IBD). As genetic susceptibility plays an important role in the etiology of IBD, we questioned how granulomatous enterocolitis and arthritis are genetically controlled in an experimental animal model displaying both conditions.

Methods—Chronic intestinal and systemic inflammation was induced by intramural injection of peptidoglycan-polysaccharide (PG-PS) polymers in the ileocaecal region of female F2 progeny derived from susceptible LEW and resistant F344 rats. Animals were followed for 24 days after injection and phenotyped by evaluating gross gut lesions, liver weight and granulomas, hematocrit, white blood cell count, and change in rear ankle joint diameters. Coinheritance of the phenotypic parameters with polymorphic DNA markers was analyzed by genome-wide quantitative trait locus (QTL) analysis.

Results—Linkage analysis revealed significant QTLs for enterocolitis and/or related phenotypes (liver granulomas, white blood cell count) on chromosomes 8 and 17. The QTL on chromosome 8 also showed suggestive linkage to arthritis. Significant QTLs for arthritis were detected on chromosomes 10, 13, 15, and 17. Analyses of the modes of inheritance showed arthritogenic contributions by both parental genomes. In addition, several other loci with suggestive evidence for linkage to one or several phenotypes were found.

Conclusion—Susceptibility to PG-PS-induced chronic intestinal and systemic inflammation in rats is under complex multigenic control in which the genetic loci regulating arthritis are largely different from those controlling enterocolitis. Possible candidate genes within these QTL (including *Tnfrsf11a/RANK*, *Gpc5*, *Il2ra*, and *Nfrkb*) are also implicated in the respective human diseases.

Corresponding Author: Andre Bleich, DVM, PhD, Institute for Laboratory Animal Science and, Central Animal Facility, Hannover Medical School, Carl-Neuberg-Str. 1, 30625 Hannover, Germany, Phone: +49 511 532 8714, Fax: +49 511 532 3710, bleich.andre@mh-hannover.de.

⁴Current institution: Biomedical Diagnostics, Hannover, Germany

[#]These authors contributed equally.

Keywords

Animal models of IBD; Arthritis; Extraintestinal manifestation in IBD; Genetics; Mucosal Immunology; Pathology; Quantitative trait

Introduction

Inflammatory bowel diseases (IBD) in humans encompass a heterogeneous collection of chronic inflammatory conditions, including Crohn's disease (CD) and ulcerative colitis (UC). Both CD and UC are not restricted to the gastrointestinal tract and often involve other organs such as joints, skin, liver, and eyes. Up to 47% of the patients with IBD have extraintestinal manifestations, 1 among which inflammatory arthropathies (such as peripheral arthritis, ankylosing spondylitis, and sacroiliitis) are most common with a prevalence ranging between 7% and 25%.^{2,3}

Although progress was made in identifying predisposing genetic factors such as polymorphisms in the *NOD2/CARD15* gene,^{4,5} development of IBD entails complex and as yet poorly understood interactions between host genetics and environmental influences.⁶ A valuable experimental model of IBD for the analysis of host genetic factors is the peptidoglycan-polysaccharide (PG-PS)-induced rat model of chronic intestinal and systemic inflammation. In this model, injection of PG-PS polymers derived from group A streptococci into the intestinal wall of genetically susceptible rats induces acute inflammation at the injection site followed by a spontaneously reactivating granulomatous enterocolitis and systemic inflammation similar to extraintestinal manifestations of IBD.⁷⁻⁹ This susceptibility to spontaneous reactivation is restricted to Lewis (LEW) and Sprague-Dawley rats and does not appear in Fischer 344 (F344) and Buffalo rats. Female LEW rats, the highest responders, develop acute intestinal inflammation that peaks 1–2 days after PG-PS injection, gradually decreases over the next 10 days, and spontaneously reactivates beginning on day 14 to produce a chronic, granulomatous fibrotic transmural inflammation that is T cell-mediated and accompanied by extraintestinal manifestations of erosive arthritis, granulomatous hepatitis, normochromic anemia, and leukocytosis that persists for at least 16 weeks.

The aim of this study was to identify chromosomal locations that determine genetic susceptibility to chronic enterocolitis and systemic inflammation in PG-PS-treated female rats of an F2 population segregating for LEW and F344 alleles by quantitative trait locus (QTL) analysis. Both strains express the same haplotypes of major histocompatibility complex (MHC) genes involved in antigen presentation (MHC class Ia and class II),¹⁰ which facilitated the analysis of non-MHC determinants of inflammatory susceptibility in this study.

Material and Methods

Animals

Susceptible specific pathogen free (SPF) LEW rats (females) and resistant F344 rats (males) obtained from Charles River (Raleigh, North Carolina) were crossed and F1 hybrids intercrossed to produce 168 female (LEW×F344)F2 segregants under SPF conditions at the University of North Carolina at Chapel Hill.

All rat experiments were conducted in accordance with the standards of the National Institutes of Health's *Guide for the Care and Use of Laboratory Animals* and approved by the University of North Carolina Institutional Animal Care and Use Committee.

Induction of enterocolitis and systemic inflammation

PG-PS was prepared from group A, type 3, strain D58 streptococci (*Streptococcus pyogenes*) as previously described;^{9,11} several sonicates were pooled so that all rats obtained the same homogenous preparation. Female F2 rats (150–160 g body weight) were anesthetized with 80 mg/kg body weight ketamine and 0.15 mg/kg acepromazine maleate intramuscularly. Their intestines were exposed by laparotomy using aseptic technique and 0.05 ml PG-PS suspension (45 mg/kg dry weight [15 mg rhamnose/kg]) was injected intramurally into 7 sites (two Peyer's patches in the distal ileum, two locations at the junction between the mesentery and terminal ileum, and three locations in the cecum including the lymphoid aggregate at the cecal tip). The abdominal cavity was closed and rats were allowed free access to food and water. Rats were followed for 24 days after treatment to allow full development of the chronic phase of inflammation and subsequently euthanized by CO₂-inhalation and exsanguination.

Phenotyping

Arthritis—Joint diameters (in millimeters) of the rear ankles were measured on day 0, 17, 21, and 24 of treatment and differences to pre-injection values calculated. Furthermore, differences in diameter of both ankles at day 24 compared to values before treatment were summed up.

Gross gut score—At necropsy, enterocolitis was assessed based on a validated 0–4 grading system by determining cecal granulomas, cecal wall thickening, mesenteric contraction and adhesions, resulting in a maximal score of 16.7⁹

In addition, livers were weighed (mg liver/g body weight) and granulomas in the livers assessed using a 0–4 scoring system. Cardiac blood samples were analyzed for hematocrit (%) and white blood cell count (10³/mm³).

Genotyping

Genomic DNA was isolated from frozen auricular or kidney tissues using the QIAamp DNA Mini Kit (Qiagen, Hilden, Germany) following the manufacturer's protocol. DNAs were genotyped by PCR amplification of 130 microsatellite markers polymorphic between LEW and F344 strains (*D1Rat186, D1Rat313, D1Rat268, D1Rat350, D1Rat66, D1Rat70, D1Rat169, D1Rat90, D2Rat201, D2Mit6, D2Rat135, D2Rat26, D2Rat147, D2Rat236, D2Rat62, D2Rat69, D2Rat342, D2Rat167, D2Rat41, D2Rat99, D3Rat82, D3Rat108, D3Rat166, D3Rat5, D3Rat3, D4Rat2, D4Rat153, D4Rat48, D4Rat137, D4Mit24, D4Rat112, D5Rat126, D5Rat82, D5Mit10, D5Rat85, D5Rat30, D5Rat93, D5Rat49, D6Rat68, D6Rat135, D6Rat165, D6Rat160, D7Rat63, D7Rat113, D7Rat107, D7Rat24, D7Rat99, D7Rat4, D7Mgh9, D7Rat26, D7Rat44, D7Mgh3, D7Rat81, D7Rat153, D7Rat150, D8Rat77, D8Arb6, D8Rat156, D8Rat129, D8Rat119, D8Rat105, D8Rat164, D8Rat99, D8Rat159, D8Rat16, D9Rat162, D9Rat41, D9Rat19, D9Rat4, D9Rat1, D10Rat218, D10Rat46, D10Rat45, D10Rat164, D10Rat26, D10Rat142, D10Rat15, D10Rat108, D10Rat37, D10Rat32, D10Rat98, D10Rat155, D10Mgh5, D11Rat11, D11Rat6, D11Arb4, D11Rat56, Kng, D12Rat4, D12Mit4, D12Rat20, D13Rat113, D13Rat26, D13Rat131, D13Rat7, D13Rat120, D13Arb8, D14Rat78, D14Rat77, D14Rat15, D14Rat18, D14Rat49, D15Rat66, D15Rat123, D15Mgh8, D15Rat106, D15Rat155, D16Rat102, D16Rat53, D16Rat15, D17Rat8, D17Rat151, D17Rat65, D17Rat11, D17Rat15, D17Mgh5, D17Rat89, D17Rat62, D18Rat17, D18Rat61, D18Rat5, D19Rat82, D19Rat12, D19Rat64, D20Rat46, D20Rat34, D20Arb10, DXRat82, DXRat43, DXRat104*). Marker positions were taken from the Rat Genome Database (www.rgd.mcw.edu), primer sequences from The Jackson Laboratory's online Mouse Genome Informatics resource (www.informatics.jax.org).

PCR reaction volume was 12 μ l which contained 50 ng DNA, 0.14 μ M of each primer (Roth, Karlsruhe, Germany), 12.5 mM Tris-HCl (pH 8.3), 62.5 mM KCl, 2.5 mM MgCl₂, 0.52 mM of each dNTP, 3 \times MasterAmp™ PCR enhancer, and 0.5 U of AmpliTherm™ DNA polymerase (Epicentre Technologies, Madison, WI). Thirty-five PCR cycles, consisting of 15 sec at 94 °C, 1 min at 55 °C, and 2 min at 72 °C, preceded by an initial denaturation step of 4 min at 95 °C and followed by a final extension step of 7 min at 72 °C, were performed in 96-well microtiter plates using a PTC-200 thermal cycler (MJ Research, Watertown, MA). For some markers, modifications of the protocol, primarily of the MgCl₂ concentration, were performed to optimize reactions. PCR products were analyzed by electrophoresis on 3% (w/v) NuSieve™ agarose gels (Bioproducts, Rockland, ME) containing GelStar (Biozym, Hess. Oldendorf, Germany) and visualized under UV light.

Statistical and QTL analyses

Spearman rank correlation analysis was used to determine the relationship between the traits under study. In addition, data were analyzed by factor analysis using a principal components solution with orthogonal rotation (varimax) of the factor matrix. This method ensures that the extracted factors are independent of one another and should, therefore, reflect separate processes. The varimax algorithm was chosen because this algorithm attempts to minimize the number of variables that have high loadings (see hereafter) on a factor. This approach should enhance the interpretability of the factors. The sampling adequacy was measured with the Kaiser-Meyer-Olkin measure (should be greater than 0.5). The Bartlett's test of sphericity was used for testing whether the correlation was appropriate for factor analysis. Factor pattern matrices were identified using a combination of the Kaiser criterion (factor must have eigenvalues ≥ 1) and the Scree test (on a simple line plot, the point of inflection of a plot of the eigenvalues from largest to smallest). The factor loading of each item indicates how well this item correlates with the factor; thus a loading of ± 1.0 indicates a perfect (positive/negative) correlation, whereas a loading of less than 0.6 would suggest that the item is rather weakly linked to the factor. Statistical significance was defined as $p \leq 0.05$.

The location of the QTLs affecting the traits was determined by using the MapQTL computer package 12. Both the interval mapping module (for normally distributed transformed enterocolitis-related and arthritis-related phenotypes)¹³ and the non-parametric mapping module (only for enterocolitis-related phenotypes)¹⁴ were used. The Kolmogorov-Smirnov one-sample test was used to check normality of the traits. The non-normally distributed traits were transformed to a normal distribution¹⁵ using the following transformations: *i*) logarithmic ($y = 10 \log[x + a]$), *ii*) logistic ($y = [x + a]/[b - x]$) or *iii*) inverse function ($y = 1/[x + a]$); where y is the transformed trait value, x is the original trait value and a and b are constants. Application of the interval mapping module on the transformed traits is then straightforward.

Results were expressed as Lod scores for normally distributed traits and Kruskal-Wallis test statistics for non-normally distributed traits. Lod score thresholds to achieve the genome-wide significance levels of 5% (significant linkage) were, as proposed by Lander and Kruglyak,¹⁶ 4.3 when no model of gene action was specified ("free" genetics), 3.4 when gene action was restricted to recessive or dominant models, and 3.3 when gene action was restricted to an additive model. For suggestive linkage, Lod score values were 2.8 ("free" genetics), 2.0 (recessive or dominant) and 1.9 (additive), respectively. For the non-parametric approach $p \leq 0.01$ and $p \leq 0.005$ were considered to indicate suggestive and significant linkage, respectively. Whenever a QTL was found or suggested using the MapQTL software, Student's *t* tests (normally traits) or Median test (non-normally distributed traits) were performed for the markers flanking the peak of the QTL or at the peak of the QTL. In case of interval mapping, the mode of inheritance was chosen as free,

additive, dominant or recessive according to the significance of differences in the mean values of the traits between rats that were homozygous LEW, heterozygous LEW:F344 and homozygous F344.

Results

Correlations and factor analysis

Positive correlations were seen between each of the following traits: gross gut score (enterocolitis), liver weight, liver granulomas, and white blood cell count, with Spearman correlation coefficients (r_s) ranging between 0.76 and 0.85 ($p < 0.0001$). Negative correlations were observed between all traits mentioned above and hematocrit ($r_s = -0.57$ to -0.77 ; $p < 0.0001$). Because of these high correlations, these traits were designated “enterocolitis-related phenotypes”. No correlation was observed between enterocolitis-related and arthritis-related (i.e. increase in joint diameter) phenotypes, except for a weak correlation between gross gut score and sum of increase in joint diameter of the right and left rear ankle on day 24 ($r_s = 0.16$; $p = 0.0389$).

The factor analysis included the following parameters: gross gut score, liver weight, liver granulomas, white blood cell count, hematocrit and the increase in joint diameters (days 17, 21 and 24; left and right rear ankle). A specific assumption for a factor analysis is that the parameter should not be fully derived from one or more of the other included parameters. Therefore, sum of increase in joint diameter of left and right rear ankles (on day 24) was not included. Two clear factors emerged accounting for 77.1% of the total variance (Table 1). Factor 1 explained 48.3% of the total variance and appeared to reflect enterocolitis, whereas factor 2 explained 28.8% and reflected arthritis.

QTL analyses

All traits were non-normally distributed in the F_2 population (not shown); therefore, transformation to a normal distribution was applied for interval mapping (Table 2).

Enterocolitis-related phenotypes

Significant and suggestive QTLs for enterocolitis-related phenotypes calculated by interval mapping and Kruskal-Wallis tests are shown in Table 3. Significant QTLs were detected on chromosome (chr.) 8 and 17, all derived from the LEW strain. On chr. 8, a significant contribution was seen for a locus around 26–29 cM to gross gut score (as determined by interval mapping and Kruskal-Wallis test), liver granulomas, and white blood cell count (both determined by Kruskal-Wallis tests) in a recessive manner, as well as a suggestive contribution to liver weight and hematocrit. On chr. 17, a significant QTL for liver granulomas was located at 69 cM (Kruskal-Wallis test). Furthermore, suggestive QTLs were detected on chr. 1 for hematocrit and on chr. 5 and 7 for white blood cell count. Taken together, the chr. 8 locus, explaining 10.2% of the genetic variance of the gross gut score and 9.0% of the genetic variance of liver granulomas and white blood cell count, has the most important effect on enterocolitis-related phenotypes, followed by a QTL on chr. 17 that explains 8.4% of the genetic variation of liver granulomas.

Arthritis-related phenotypes

Significant and suggestive arthritogenic QTLs are shown in Table 4 and Table 5. Significant QTLs were detected on chr. 10, 13, and 15 (with arthritogenic contributions from the LEW genome), and on chr. 17 (with an arthritogenic contribution from the F344 genome). A locus with a peak Lod score at 69.0 cM on chr. 10 was associated with an increase in joint diameter of the right ankle on days 17 and 21 in a recessive manner, and a locus with a peak at 76 cM was associated with an increase in diameter of the left ankle on day 21 as well as

the summed increase of the left and right ankle on day 24 in a dominant fashion. The LEW allele of this QTL explained up to 18.4% of the genetic variance, showing a major contribution of this QTL to arthritis susceptibility. In addition, a QTL for arthritis of the left ankle on day 24 peaked at 70 cM and showed a dominant mode of inheritance. The presence of multiple peaks on chr. 10 indicates that several genetic factors on this chromosome may contribute to arthritis susceptibility (Fig. 1). Proximal chr. 13 (peak Lod scores between 2.0 and 7.0 cM) contributed to arthritis susceptibility in a dominant fashion and explained up to 12.8 % of the genetic variance of arthritis-related traits. A QTL at 87.0 cM on chr. 15 showed significant linkage and a second locus at 55.0 cM suggestive linkage to arthritis of the left ankle on day 17. The first was inherited in a recessive, the second in a dominant manner. A QTL on chr. 17 was significantly associated to arthritis of the left ankle on day 17, 21, and 24 as well as the summed up increase in joint diameter on day 24 and peaked between 51.0 and 52 cM. Suggestive linkage was identified for the same locus to increases of joint diameters of the right ankle on all three days. Additional suggestive linkage to arthritis-related phenotypes was detected on chr. 2, 7, 8, and 20 (Table 5).

Discussion

Inflammatory arthropathies are common extraintestinal manifestations of IBD. As genetic susceptibility plays an important role in the etiology of IBD, we questioned how chronic granulomatous enterocolitis and arthritis are genetically controlled in an experimental model displaying both conditions, the PG-PS-induced rat model of chronic intestinal and systemic inflammation. In this model, PG-PS is injected intramurally into different locations of the gut. As the response to these bacterial polymers is different between LEW (susceptible) and F344 (resistant) rats, these two inbred strains were chosen to breed a segregating F2 population that was used for QTL analysis. In addition, both strains express the same haplotypes of major histocompatibility complex (MHC) genes involved in antigen presentation (MHC class Ia and class II) 10, which facilitates the analysis of non-MHC determinants of inflammatory susceptibility. In humans, the MHC locus accounts for approximately 50% of familial aggregation of rheumatoid arthritis together with *PTPN22*.¹⁷ The *Ptpn22* gene is located on rat chr. 2 but not within the region containing the suggestive QTL identified in this study.

Linkage analysis revealed that susceptibility to enterocolitis and arthritis is under complex multigenic control. Interestingly, QTLs determining susceptibility to arthritis were largely different from those controlling enterocolitis and correlated phenotypes (liver weight and granulomas, anemia, leukocytosis). It should be noted that some QTLs may have been missed or had less significance in our study because only gross phenotypic measures, specifically measurement of joint diameters and gross gut score (and no histology), were taken. This is corroborated by a recent study which shows that detailed histologic phenotyping enhances power to detect colitis QTLs in mice.¹⁸ Our results indicate that genetic factors that modulate enterocolitis are localized on chr. 8 (with peak linkage at 26–29 cM) and 17 (peak linkage 69 cM), whereas factors that contribute to arthritis susceptibility are localized on chr. 10 (69–76 cM), 13 (4–7 cM), 15 (87 cM), and 17 (51–52 cM). If suggestive QTLs are taken into account, the QTL on chr. 8 might also determine susceptibility to arthritis. The suggestive enterocolitis- and arthritis-associated QTLs on chr. 7 are probably not in linkage (3 cM vs 48–69 cM) pointing to distinct QTLs on this chromosome. The suggestive enterocolitis-related QTL affecting white blood cell count on chr. 5 maps within a locus that is known as a modifier of white blood cell count (*Wbc1*) detected previously in a QTL analysis dissecting cardiovascular phenotypes of hypertension.¹⁹ This locus also overlaps with a QTL for anti-collagen antibody titer (*Ciaa5*) in the collagen-induced arthritis model.²⁰

As the chr. 8 QTL shows association to both enterocolitis and arthritis phenotypes, the underlying gene likely plays a general role in inflammatory mechanisms. The peak of the QTL on chr. 8 maps proximal to an unnamed QTL with suggestive linkage to collagen-induced arthritis, *Cia6*, and *Pia14*;²¹ the human orthologous region contains *RA19*.²² An obvious candidate gene within the peak linkage is *Nfrkb* (nuclear factor related to kappa B). The role of *Nfrkb* in IBD has been well described and a genetic association with intestinal inflammation has been demonstrated in human ulcerative colitis²³ and has been implicated in experimental colitis in mice.²⁴ *Nfrkb* is upregulated in inflammatory processes and has been originally identified to bind to a related variant of the kappa B site that regulates interleukin-2 receptor alpha-chain (*Il2ra*) gene expression, a critical event in T-cell activation.²⁵ The rat *Il2ra* gene is located on chr. 17 within a region that showed association with colitis and arthritis phenotypes in our study. These loci are spaced approximately 15 cM apart. Therefore, it remains to be determined if a common QTL controls susceptibility to both diseases. In humans, variants around the *IL2RA* gene showed disease association in a linkage study that combined rheumatoid arthritis and type 1 diabetes¹⁷, and the linkage to arthritis was replicated in a subsequent meta-analysis.²⁶ The proximal part of the QTL interval also overlaps with a region that maps to chr. 1 in humans and contains the QTL *RA2*.²⁷ The IL-2 receptor (CD25) is involved in regulation of regulatory T cells,²⁸⁻²⁹ and deletion of IL-230 or IL-2RA31-32 in mice leads to chronic colitis, hemolytic anemia and hepatobiliary disease.

Our approach enabled us to reproduce existing arthritis QTLs on chr. 10 and to identify new ones on chr. 13, 15, and 17. It is likely that more than one genetic factor determines arthritis susceptibility on chr. 10, as several peaks were observed at closely linked loci and were either inherited in a recessive or dominant manner depending on phenotype. This is in concordance with previous linkage analyses that identified multiple loci contributing to arthritis susceptibility on this chromosome. QTLs determining susceptibility to collagen-, oil- and squalene-, pristane-, and mycobacterial adjuvant-induced arthritis have been identified on chr. 10 using different crosses and/or substitution mapping [reviewed in Joe²¹]. The QTL identified in this study is located proximal to *Cia5/Cia20* and overlaps partially or completely with *Cia16*, *Cia21-23*, *Oia4*, *Aia5*, *Pia10*, *Pia26*, and *Ciaa2*.²⁰⁻²²⁻³³⁻³⁶

The chr. 13 linkage to arthritis has not been previously detected in rats. Human homologous regions map either to chr. 2 [slightly overlapping with *OSTEAR1137*] or chr. 18, the latter of which contains *RA30*.²⁷ An obvious candidate in this region is the *Tnfrsf11a* (tumor necrosis factor receptor superfamily, member 11a) gene that is also known as RANK (receptor activator of Nfkb). Besides regulating T-cell/dendritic cell interaction and lymph node formation, the RANK/RANKL (L)/osteoprotegerin (OPG) system is a key regulator of bone remodelling. Its relevance in diseases with altered bone metabolism has been well investigated, e.g. in osteoporosis, Paget's disease, and rheumatoid arthritis.³⁸ Excessive expression of RANKL induced by activated T-cells contributes to osteoclastogenesis and likely contributes to joint destruction in rheumatoid arthritis and erosive arthritis in the PG-PS arthritis model; moreover, experimental manipulation of the RANK/RANKL/OPG system prevented bone loss and cartilage destruction in animal models of arthritis.³⁸⁻⁴¹

The QTL on chr. 15 is located distal to a previously described (unnamed) locus with suggestive linkage to mycobacterial adjuvant-induced arthritis.²¹ The peak marker is located within the glypican (*Gpc5*) gene. The human *GPC5* gene on chr. 13 has been implicated to play a role in osteoarthritis development via cartilage degeneration, which was identified by comparing gene expression in intact versus damaged regions of osteoarthritis cartilage.⁴² Furthermore, a polymorphism of the human *GPC5* gene is associated to

symptoms including arthritis following human parvovirus B19 infection.^{43,44} Glypicans are cell surface heparan sulfate proteoglycans that are linked with integrin and TGF β signalling and play various roles in development and differentiation.⁴⁵ TGF β is a key mediator of regulatory T cell activity.²⁹

Reactive arthritis is a well known extraintestinal manifestation of IBD. As the PG-PS-induced rat model provides the opportunity to mirror both arthritis and enterocolitis, it prompted us to investigate if susceptibility to enterocolitis and arthritis is controlled by common genetic factors or rather independently in this model. Common loci were likely identified on chr. 17 and chr. 8 (if the suggestive linkage to arthritis of the latter is taken into account) indicating the involvement of shared mechanisms in susceptibility to both inflammatory conditions. Candidate genes identified in these regions (*Nfrkb* and *Il2ra*) are in line with this hypothesis. However, with the observation of multiple independent loci, our study also demonstrates that both conditions are largely regulated by distinct genetic factors. The linkage on chr. 10 with PG-PS-induced arthritis is in accordance with similar findings in several other rat models of arthritis, showing that this chromosome contains important regulators of arthritis susceptibility in the rat. The majority of QTLs associated with arthritis phenotypes in this study, however, are unique to the PG-PS-induced model. As these QTLs contain interesting candidate genes (*Tnfrsf11a/RANK*, *Gpc5*, *Il2ra*, *Nfrkb*) that are also implicated in human diseases, our model might be of help to elucidate the human situation.

Acknowledgments

We gratefully acknowledge the excellent technical assistance of Ina Köhn and Anna Smoczek.

This work was supported by the Crohn's and Colitis Foundation of America (to M.M. and R.B.S.) and NIH grant RO1 DK40249.

References

1. Mendoza JL, Lana R, Taxonera C, et al. Extraintestinal manifestations in inflammatory bowel disease: differences between Crohn's disease and ulcerative colitis. *Med Clin (Barc)*. 2005; 125:297–300. [PubMed: 16159555]
2. Veloso FT, Carvalho J, Magro F. Immune-related systemic manifestations of inflammatory bowel disease. A prospective study of 792 patients. *J Clin Gastroenterol*. 1996; 23:29–34. [PubMed: 8835896]
3. De Vos M. Review article: joint involvement in inflammatory bowel disease. *Aliment Pharmacol Ther*. 2004; 20 Suppl 4:36–42. [PubMed: 15352892]
4. Hugot JP, Chamaillard M, Zouali H, et al. Association of *NOD2* leucine-rich repeat variants with susceptibility to Crohn's disease. *Nature*. 2001; 411:599–603. [PubMed: 11385576]
5. Ogura Y, Bonen DK, Inohara N, et al. A frameshift mutation in *NOD2* associated with susceptibility to Crohn's disease. *Nature*. 2001; 411:603–606. [PubMed: 11385577]
6. Sartor RB. Microbial influences in inflammatory bowel diseases. *Gastroenterology*. 2008; 134:577–594. [PubMed: 18242222]
7. Sartor RB, Cromartie WJ, Powell DW, et al. Granulomatous enterocolitis induced in rats by purified bacterial cell wall fragments. *Gastroenterology*. 1985; 89:587–595. [PubMed: 3926593]
8. Sartor RB, DeLa Cadena RA, Green KD, et al. Selective kallikrein-kinin system activation in inbred rats differentially susceptible to granulomatous enterocolitis. *Gastroenterology*. 1996; 110:1467–1481. [PubMed: 8613052]
9. McCall RD, Haskill S, Zimmermann EM, et al. Tissue interleukin 1 and interleukin-1 receptor antagonist expression in enterocolitis in resistant and susceptible rats. *Gastroenterology*. 1994; 106:960–972. [PubMed: 8144001]
10. Hedrich, HJ. Mutant genes and polymorphic loci of the laboratory rat. In: Hedrich, HJ., editor. *Genetic monitoring of inbred strains of rats*. Stuttgart: Gustav Fischer Verlag; 1990. p. 289-409.

11. Stimpson, SA.; Schwab, JH. Chronic remittent erosive arthritis induced by bacterial peptidoglycan-polysaccharide structures. In: Chang, JY.; Lewis, AJ., editors. Pharmacological methods in the control of inflammation. New York: Alan R. Liss; 1989. p. 381-394.
12. Van Ooijen, JW.; Maliepaard, C. MapQTLTM version 3.0: Software for the calculation of QTL postions on genetic maps. Wageningen: CPRO-DLO; 1996.
13. Lander ES, Botstein D. Mapping Mendelian factors underlying quantitative traits using RFLP linkage maps. *Genetics*. 1989; 121:185–199. [PubMed: 2563713]
14. Kruglyak L, Lander ES. A nonparametric approach for mapping quantitative trait loci. *Genetics*. 1995; 139:1421–1428. [PubMed: 7768449]
15. Petrie, A.; Watson, P. Statistics for veterinary and animal science. London: Blackwell Science; 1999.
16. Lander E, Kruglyak L. Genetic dissection of complex traits: guidelines for interpreting and reporting linkage results. *Nat Genet*. 1995; 11:241–247. [PubMed: 7581446]
17. The Wellcome Trust Case Control Consortium. Genome-wide association study of 14,000 cases of seven common diseases and 3,000 shared controls. *Nature*. 2007; 447:661–678. [PubMed: 17554300]
18. Bleich A, Mähler M, Most C, et al. Refined histopathologic scoring system improves power to detect colitis QTL in mice. *Mamm Genome*. 2004; 15:865–871. [PubMed: 15672590]
19. Moreno C, Dumas P, Kaldunski ML, et al. Genomic map of cardiovascular phenotypes of hypertension in female Dahl S rats. *Physiol Genomics*. 2003; 15:243–257. [PubMed: 14532335]
20. Furuya T, Salstrom JL, McCall-Vining S, et al. Genetic dissection of a rat model for rheumatoid arthritis: significant gender influences on autosomal modifier loci. *Hum Mol Genet*. 2000; 9:2241–2250. [PubMed: 11001927]
21. Joe B. Quest for arthritis-causative genetic factors in the rat. *Physiol Genomics*. 2006; 27:1–11. [PubMed: 16804090]
22. Rat Genome Database. Medical College of Wisconsin, Milwaukee, Wisconsin. [Accessed August 2008.]. Available at: <http://rgd.mcw.edu/>.
23. Karban AS, Okazaki T, Panhuysen CI, et al. Functional annotation of a novel NFKB1 promoter polymorphism that increases risk for ulcerative colitis. *Hum Mol Genet*. 2004; 13:35–45. [PubMed: 14613970]
24. Beckwith J, Cong Y, Sundberg JP, et al. *Cdcs1*, a major colitogenic locus in mice, regulates innate and adaptive immune response to enteric bacterial antigens. *Gastroenterology*. 2005; 129:1473–1484. [PubMed: 16285949]
25. Adams BS, Leung KY, Hanley EW, et al. Cloning of R kappa B, a novel DNA-binding protein that recognizes the interleukin-2 receptor alpha chain kappa B site. *New Biol*. 1991; 3:1063–1073. [PubMed: 1777480]
26. Seielstad M, Padyukov L, Ke X, Ding B, Tantoso E, Ong THR, et al. Combined Analysis of Three Genome-wide Scans Reveals Additional Loci Associated with Rheumatoid Arthritis. *Clinical Immunology*. 2008; 127 Suppl 1:S41. (Abstract).
27. Jawaheer D, Seldin MF, Amos CI, et al. A genomewide screen in multiplex rheumatoid arthritis families suggests genetic overlap with other autoimmune diseases. *Am J Hum Genet*. 2001; 68:927–936. [PubMed: 11254450]
28. Lan RY, Selmi C, Gershwin ME. The regulatory, inflammatory, and T cell programming roles of interleukin-2 (IL-2). *J Autoimmun*. 2008; 31:7–12. [PubMed: 18442895]
29. Askenasy N, Kaminitz A, Yarkoni S. Mechanisms of T regulatory cell function. *Autoimmun Rev*. 2008; 7:370–375. [PubMed: 18486924]
30. Sadlack B, Merz H, Schorle H, et al. Ulcerative colitis-like disease in mice with a disrupted interleukin-2 gene. *Cell*. 1993; 75:253–261. [PubMed: 8402910]
31. Willerford DM, Chen J, Ferry JA, et al. Interleukin-2 receptor alpha chain regulates the size and content of the peripheral lymphoid compartment. *Immunity*. 1995; 3:521–530. [PubMed: 7584142]
32. Hsu W, Zhang W, Tsuneyama K, et al. Differential mechanisms in the pathogenesis of autoimmune cholangitis versus inflammatory bowel disease in interleukin-2Ralpha(–/–) mice. *Hepatology*. 2009; 49:133–140. [PubMed: 19065673]

33. Joe B, Cannon GW, Griffiths MM, et al. Evaluation of quantitative trait loci regulating severity of mycobacterial adjuvant-induced arthritis in monocongenic and polycongenic rats: identification of a new regulatory locus on rat chromosome 10 and evidence of overlap with rheumatoid arthritis susceptibility loci. *Arthritis Rheum.* 2002; 46:1075–1085. [PubMed: 11953987]
34. Olofsson P, Holmberg J, Pettersson U, et al. Identification and isolation of dominant susceptibility loci for pristane-induced arthritis. *J Immunol.* 2003; 171:407–416. [PubMed: 12817024]
35. Brenner M, Meng HC, Yarlett NC, et al. The non-MHC quantitative trait locus *Cia5* contains three major arthritis genes that differentially regulate disease severity, pannus formation, and joint damage in collagen- and pristane-induced arthritis. *J Immunol.* 2005; 174:7894–7903. [PubMed: 15944295]
36. Longman RE, Remmers EF, Cannon GW, et al. Localization of genetic loci controlling antibody response to autologous collagen in rats with collagen-induced arthritis. *Arthritis Rheum.* 1996; 39 Suppl 9:S117. (Abstract).
37. Leppavuori J, Kujala U, Kinnunen J, et al. Genome scan for predisposing loci for distal interphalangeal joint osteoarthritis: evidence for a locus on 2q. *Am J Hum Genet.* 1999; 65:1060–1067. [PubMed: 10486325]
38. Loddenkemper K, Burmester GR. What is the rank of RANKL in spondylarthritis? *Arthritis Rheum.* 2008; 58:641–644. [PubMed: 18311809]
39. Vandooren B, Cantaert T, Noordenbos T, et al. The abundant synovial expression of the RANK/RANKL/Osteoprotegerin system in peripheral spondylarthritis is partially disconnected from inflammation. *Arthritis Rheum.* 2008; 58:718–729. [PubMed: 18311801]
40. Kong YY, Feige U, Sarosi I, et al. Activated T cells regulate bone loss and joint destruction in adjuvant arthritis through osteoprotegerin ligand. *Nature.* 1999; 402:304–309. [PubMed: 10580503]
41. Saidenberg-Kermanac'h N, Corrado A, Lemeiter D, et al. TNF-alpha antibodies and osteoprotegerin decrease systemic bone loss associated with inflammation through distinct mechanisms in collagen-induced arthritis. *Bone.* 2004; 35:1200–1207. [PubMed: 15542046]
42. Sato T, Konomi K, Yamasaki S, et al. Comparative analysis of gene expression profiles in intact and damaged regions of human osteoarthritic cartilage. *Arthritis Rheum.* 2006; 54:808–817. [PubMed: 16508957]
43. Kerr JR. Pathogenesis of parvovirus B19 infection: host gene variability, and possible means and effects of virus persistence. *J Vet Med B Infect Dis Vet Public Health.* 2005; 52:335–339. [PubMed: 16316396]
44. Kerr JR, Kaushik N, Fear D, et al. Single-nucleotide polymorphisms associated with symptomatic infection and differential human gene expression in healthy seropositive persons each implicate the cytoskeleton, integrin signaling, and oncosuppression in the pathogenesis of human parvovirus B19 infection. *J Infect Dis.* 2005; 192:276–286. [PubMed: 15962222]
45. De Cat B, David G. Developmental roles of the glypicans. *Semin Cell Dev Biol.* 2001; 12:117–125. [PubMed: 11292377]

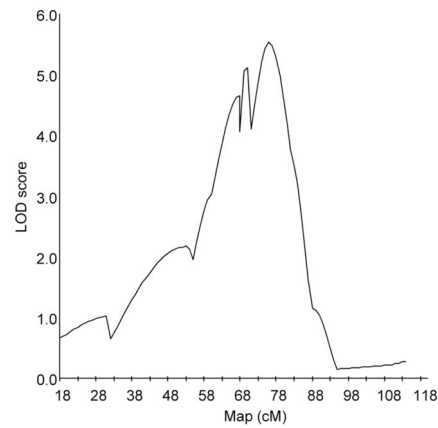


Figure 1.

Lod plot of the arthritis QTL associated with the phenotype “sum of increases in diameter of both ankles at day 24” on chr. 10. The graphical presentation of the Lod scores determined by interval mapping demonstrates the complex linkage on chr. 10 with multiple peaks.

Table 1

Orthogonal factor loadings for the measured phenotypes

Phenotypic trait	Factor 1	Factor 2
<i>Gross gut score</i>	0.916	0.131
<i>Liver weight</i>	0.926	0.168
<i>Liver granulomas</i>	0.895	0.155
<i>WBC ($10^3/\text{mm}^3$)</i>	0.849	0.057
<i>Hematocrit (%)</i>	-0.791	-0.025
Δ Joint diameter, day 17 (mm)		
<i>Left rear ankle</i>	0.035	0.831
<i>Right rear ankle</i>	0.065	0.790
Δ Joint diameter, day 21 (mm)		
<i>Left rear ankle</i>	0.117	0.889
<i>Right rear ankle</i>	0.121	0.906
Δ Joint diameter, day 24 (mm)		
<i>Left rear ankle</i>	0.132	0.875
<i>Right rear ankle</i>	0.152	0.893

The data from all female F2 mice of this study (n = 168) were subject to factor analysis. The Kaiser-Meyer-Olkin measure is 0.809, indicating a high sampling adequacy for the factor analysis. Bartlett's test for sphericity indicates that the factor model is appropriate ($p < 0.0005$). Factor loadings > 0.6 are considered to be high and are indicated in bold.

Table 2

Transformation of phenotype data for QTL analyses

Phenotypic trait	Transformation (function)
Gross gut score	$y=10\log[x/(17.00-x)]$
Liver weight	$y=10\log[x - 8.05]$
Liver granulomas	$y=10\log[(x+0.115)/(4.115-x)]$
WBC ($10^3/\text{mm}^3$)	$y=10\log[x - 4.82]$
Hematocrit (%)	$y=10\log[x - 19.74]$
Δ Joint diameter, day 17 (mm)	
Left rear ankle	$y=1/(x+0.288)$
Right rear ankle	$y=1/(x+0.232)$
Δ Joint diameter, day 21 (mm)	
Left rear ankle	$y=1/(x+0.2773)$
Right rear ankle	$y=1/(x+0.2590)$
Δ Joint diameter, day 24 (mm)	
Left rear ankle	$y=1/(x+0.2215)$
Right rear ankle	$y=1/(x+0.2111)$
Sum of left and right rear ankles	$y=1/(x+0.3749)$

WBC, white blood cell count.

Table 3

Summary of the QTLs for enterocolitis-related phenotypes in rats

Phenotypic trait	Chr.	Parametric approach ¹			Non-parametric approach		
		Model ²	Lod ³	Location ⁴	% Var. ⁵	p-value ³	Marker
Gross gut score	8	Recessive (+)	3.52	26.0 cM	10.2	≤0.005	<i>D8Rat164</i> (27.0 cM)
Liver weight	8	Additive (+)	2.43	29.0 cM	7.1	≤0.01	<i>D8Rat164</i> (27.0 cM)
Liver granulomas	8	Recessive (+)	3.21	29.0 cM	9.0	≤0.005	<i>D8Rat164</i> (27.0 cM)
	17	Dominant (+)	2.89	64.0 cM	8.4	≤0.005	<i>D17Rat62</i> (69.0 cM)
WBC (10 ³ /mm ³)	5	Recessive (-)	2.51	82.0 cM	10.1	≤0.01	<i>D5Rat30</i> (73.0 cM)
	7					≤0.01	<i>D7Rat63</i> (3.0 cM)
	8	Recessive (+)	3.21	29.0 cM	9.0	≤0.005	<i>D8Arb6</i> (31.0 cM)
Hematocrit (%)	1					≤0.01	<i>D1Rat169</i> (142.0 cM)
	8	Recessive (-)	2.06	27.0 cM	5.5		

¹ Interval mapping module was performed on transformed enterocolitis-related data (logistic or logarithmic transformation).

² Additive, dominant or recessive as well as plus (+) or minus (-) contribution to the trait was defined with respect to the LEW grandparent's allele.

³ Thresholds for suggestive and significant (bold) linkage are described in Material and Methods.

⁴ The location on the chromosome where the Lod score peaked.

⁵ Percentage of the genetic variance explained by the QTL. WBC, white blood cell count.

Table 4

Summary of significant QTLs (parametric approach, interval mapping) for arthritis-related phenotypes (joint diameter) in rats¹

Chr.	Δ Diameter	Model ³	Lod	Location ⁴	% Var. ⁵	
Day	Side					
10	17	Right	Recessive (+)	4.31	<i>D10Rat155</i> to <i>D10Rat26</i> (69.0 cM)	13.8
	21	Left	Dominant (+)	3.82	<i>D10Rat26</i> to <i>D10Mgh5</i> (76.0 cM)	12.6
		Right	Recessive (+)	4.87	<i>D10Rat155</i> to <i>D10Rat26</i> (69.0 cM)	15.1
	24	Left	Dominant (+)	4.92	<i>D10Rat155</i> to <i>D10Rat26</i> (70.0 cM)	14.2
		Sum	Dominant (+)	5.54	<i>D10Rat26</i> to <i>D10Mgh5</i> (76.0 cM)	18.4
13	21	Left	Dominant (+)	3.97	<i>D13Rat113</i> (7.0 cM)	10.4
	24	Left	Dominant (+)	4.62	<i>D13Rat7</i> to <i>D13Rat113</i> (4.0 cM)	12.8
15	17	Left	Recessive (+)	3.41	<i>D15Rat106</i> (87.0 cM)	8.9
17	17	Left	Dominant (-)	4.06	<i>D17Rat151</i> to <i>D17Rat89</i> (52.0 cM)	11.5
	21	Left	Dominant (-)	4.24	<i>D17Rat151</i> (51.0 cM)	11.0
	24	Left	Dominant (-)	3.68	<i>D17Rat151</i> to <i>D17Rat89</i> (52.0 cM)	10.3
		Sum	Dominant (-)	3.49	<i>D17Rat151</i> to <i>D17Rat89</i> (52.0 cM)	9.8

¹The QTL analysis was performed on transformed data; thresholds are described in Material and Methods.

²Joint diameters of the rear ankles (left, right, or sum of both sides) on day 17, 21, or 24 compared to pre-injection values (calculated differences [Δ]).

³Additive, dominant or recessive as well as plus (+) or minus (-) contribution to the trait was defined with respect to the LEW grandparent's allele.

⁴The location on the chromosome where the Lod score peaked is given in parentheses.

⁵Percentage of the genetic variance explained by the QTL.

Table 5

Summary of suggestive QTLs (parametric approach, interval mapping) for arthritis-related phenotypes (joint diameter) in rats¹

Chr.	Δ Diameter	Model ³	Lod	Location ⁴	% Var. ⁵	
Day	Side					
2	21	Left	Recessive (-)	2.9	<i>D2Mit16</i> to <i>D2Rat167</i> (54.0 cM)	8.1
	24	Left	Additive (-)	3.29	<i>D2Rat26</i> (63.0 cM)	8.6
7	17	Right	Dominant (+)	2.46	<i>D7Rat26</i> to <i>D7Rat44</i> (48.0 cM)	7.4
	21	Right	Dominant (+)	2.71	<i>D7Rat24</i> to <i>D7Rat99</i> (63.0 cM)	9.5
	24	Left	Dominant (+)	2.13	<i>D7Rat99</i> (69.0 cM)	5.7
	24	Right	Dominant (+)	2.09	<i>D7Rat24</i> to <i>D7Rat99</i> (64.0 cM)	7.1
	24	Sum	Dominant (+)	2.45	<i>D7Rat99</i> (69.0 cM)	6.5
8	24	Left	Dominant (+)	2.42	<i>D8ARb6</i> (31.0 cM)	10.3
10	17	Left	Dominant (+)	2.98	<i>D10Rat155</i> to <i>D10Rat26</i> (70.0 cM)	8.8
	24	Right	Dominant (+)	3.38	<i>D10Rat26</i> to <i>D10Mgh5</i> (76.0 cM)	12.0
13	17	Left	Dominant (+)	2.75	<i>D13Rat113</i> (7.0 cM)	7.3
	21	Right	Dominant (+)	2.29	<i>D13Rat7</i> (2.0 cM)	6.1
	24	Sum	Dominant (+)	2.3	<i>D13Rat7</i> to <i>D13Rat113</i> (4.0 cM)	6.5
15	17	Left	Dominant (+)	2.06	<i>D15Rat123</i> to <i>D15Mgh8</i> (55.0 cM)	7.5
17	17	Right	Dominant (-)	2.69	<i>D17Rat151</i> to <i>D17Mgh5</i> (43.0 cM)	7.9
	21	Right	Dominant (-)	3.22	<i>D17Rat151</i> (51.0 cM)	8.4
	24	Right	Dominant (-)	2.73	<i>D17Rat151</i> (51.0 cM)	7.2
20	17	Right	Free (H) ⁶	2.83	<i>D20Rat46</i> to <i>D20Rat34</i> (20.0 cM)	13.7
	24	Right	Free (H)	2.92	<i>D20Rat46</i> to <i>D20Rat34</i> (15.0 cM)	12.5

¹The QTL analysis was performed on transformed data; thresholds are described in Material and Methods.

²Joint diameters of the rear ankles (left, right, or sum of both sides) on day 17, 21, or 24 compared to pre-injection values (calculated differences [Δ]).

³Additive, dominant or recessive as well as plus (+) or minus (-) contribution to the trait was defined with respect to the LEW grandparent's allele.

⁴The location on the chromosome where the Lod score peaked is given in parentheses.

⁵Percentage of the genetic variance explained by the QTL.

⁶For some regions the heterozygous genotype was higher than both homozygous genotypes (heterosis effect, H). In these cases the two homozygous genotypes had an identical arthritis phenotype.